Associative Behavior and Diffusion Coefficients of Hydrophobically Modified Poly(*N*,*N*-dimethylacrylamides)

Yoshimitsu Uemura, James McNulty, and Peter M. Macdonald*

Department of Chemistry and Erindale College, University of Toronto, Toronto, Ontario, Canada M5S 1A2

Received December 1, 1994; Revised Manuscript Received March 15, 1995®

ABSTRACT: We have characterized the association behavior of a series of randomly hydrophobically-modified poly(*N*,*N*-dimethylacrylamides) having different molecular weights and different degrees of hydrophobic modification with the hydrophobic modifier octadecylpyrene. The extent of association between hydrophobes was quantified using fluorescence spectroscopy to measure excimer/monomer ratios. The consequences of this association for the diffusion of the polymer chains were measured using the pulsed-gradient spin-echo (PGSE) nuclear magnetic resonance (NMR) technique. In general, higher degrees of hydrophobic modification cause higher polymer association probabilities. Specifically, at low degrees of hydrophobic modification the associations are primarily intermolecular at all concentrations, while at high degrees of hydrophobic modification there is a crossover from primarily intramolecular to primarily intermolecular associations with increasing concentration. Network formation does not occur within the range of concentration investigated, probably because the substantial hydrophobicity of these particular hydrophobic modifiers favors smaller aggregates. In the concentration regime where intermolecular associations dominate, the most hydrophobic associating polymers form clusters consisting of four macromolecules on average.

Introduction

Associating polymers are used in many industrial applications for controlling the rheological properties of, for example, paints, coatings, and enhanced oil-recovery formulations.[1−3] They consist of a water-soluble polymer backbone to which hydrophobic modifiers are attached. The hydrophobic groups associate in a nonspecific fashion with each other and with other components of an aqueous mixture, such as latex or surfactant. As a consequence of their burgeoning industrial importance, molecular-level studies of associating polymers have begun to appear in increasing numbers. The range of experimental techniques includes dynamic light scattering,[4,5] fluorescence spectroscopy,[4,6,7] and nuclear magnetic resonance spectroscopy.[5,8−10] Simultaneously, several theoretical studies of associating polymers, generally starting from a transient network model, have been proposed and appear to have captured the essentials of the association mechanism and explained the major properties.[11−14] Nevertheless, engineering the rheological properties of such formulations remains largely an empirical process because the link between chemical structure, associative properties, and rheological behavior in such polymers still remains rather tenuous.

Two fundamentally different structural archetypes of associating polymer have emerged: the telechelic associating polymers, in which hydrophobic modifiers are located only at the ends of the water-soluble polymer backbone, and the comb-type associating polymers, in which hydrophobic modifiers are distributed randomly along the polymer backbone. The telechelic associating polymers, as exemplified by the HEUR associative thickeners,[15] form micellar clusters or "rosettes" consisting of looped polymer chains with their hydrophobic groups sequestered into a micelle-like core.[4] As the polymer concentration increases, bridging chains begin to link the rosettes into supraclusters, eventually forming a network spanning the solution. The comb-type associating polymers, on the other hand, experience predominantly intramolecular associations at low polymer concentrations, with a transition to intermolecular association occurring at a critical concentration which depends on molecular details such as the length of the hydrophobic modifier and the degree of hydrophobic modification.[16]

Fluorescence studies have yielded information regarding the degree of association, the viscosity within the association site, and the aggregation number of the micellar clusters formed by both telechelic and comblike associating polymers.[4,6,7] PGSE NMR is employed to measure diffusion coefficients[17] and, by inference, the size of the diffusing species in an associated network, as well as the time scale for relaxation in the polymer network.[5,8−10] Very different behavior is anticipated for the concentration dependence of the diffusion coefficients for the two different associating polymer archetypes.[11] To the best of our knowledge, no PGSE NMR studies of comblike associating polymers have yet appeared.

We describe here the results of combined fluorescence and PGSE NMR studies of a series of poly(*N*,*N*-dimethylacrylamides), hydrophobically modified with 1-(1-pyrenyl)octadecyl groups (HM-PDMAM) distributed comblike, in a random fashion along the PDMAM backbone. Fluorescence spectroscopy of the pyrene moiety is used to characterize the degree of association, and PGSE NMR is used to measure polymer diffusion coefficients.

Experimental Section

Polymer Synthesis. Our general synthetic strategy for preparing hydrophobically-modified poly(*N*,*N*-dimethylacrylamide) follows closely that described by Winnik.[18] The final product, as shown in Figure 1, is a random copolymer of *N*,*N*-dimethylacrylamide plus *N*-[1-(1-pyrenyl)octadecyl]acrylamide. In outline, the synthesis involves first preparing a copolymer of *N*,*N*-dimethylacrylamide (NMAM) plus *N*-(acryloxy)succinimide (NASI). Next, the hydrophobic moieties are introduced by replacing the oxysuccinimides with 1-(1-pyrenyl)octadecylamine. Finally, any remaining oxysuccinimide moieties are

* To whom correspondence should be addressed.
® Abstract published in *Advance ACS Abstracts,* May 1, 1995.

0024-9297/95/2228-4150$09.00/0

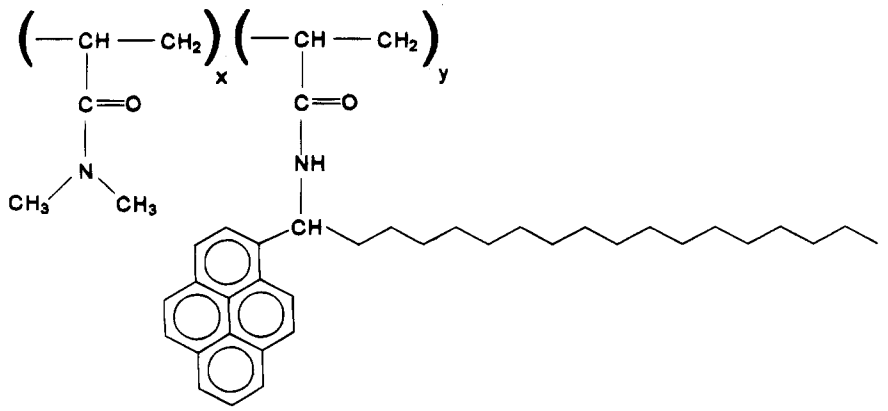

Figure 1. Structure of hydrophobically-modified poly(*N,N*-dimethylacrylamide) or HM-PDMAM.

removed by the addition of dimethylamine. The overall molecular weight is controlled by modulating the initial polymerization conditions, while the degree of hydrophobic modification is a function of the ratio of NMAM to NASI copolymerized.

Materials. Pyrene, aluminum chloride, stearoyl chloride, *N,N*-dimethylacrylamide, *N*-hydroxysuccinimide, acryloyl chloride, sodium borohydride, and lithium aluminum hydride were obtained from Aldrich Chemical Co. (Milwaukee, WI). Dry diethyl ether, 1,2-dichloroethane, tetrahydrofuran, *tert*-butyl alcohol, 1-propanol, and ethanol were obtained from BDH (Mississauga, ON). AIBN (1,1′-azo*bis*(isobutyronitrile)) was a kind gift of Dr. F. M. Winnik of the Xerox Research Centre of Canada (Mississauga, ON).

1-(1-Pyrenyl)octadecylamine and *N*-(Acryloxy)succinimide. 1-(1-Pyrenyl)octadecylamine was prepared indirectly by the lithium aluminum hydride promoted reduction in dry diethyl ether of the oxime obtained from condensation of 1-(1-pyrenyl)octadecanone with hydroxylamine in pyridine/1,2-dichloroethane.[19] The ketone 1-(1-pyrenyl)octadecanone was prepared via a Friedel–Crafts acylation of pyrene with stearoyl chloride in 1,2-dichloroethane.[20] *N*-(acryloxy)succinimide was prepared by reacting acryloyl chloride with *N*-hydroxysuccinimide as per the literature.[18] The identity of the desired products was confirmed by ^{1}H NMR, Fourier transform infrared, and mass spectroscopies.

***N,N*-Dimethylacrylamide–*N*-(Acryloxy)succinimide Copolymer.** The molecular weight of the *N,N*-dimethylacrylamide–*N*-(acryloxy)succinimide copolymer was controlled by varying the ratio of 1-propanol to *tert*-butyl alcohol used as the polymerization solvent. (The 1-propanol/*tert*-butyl alcohol ratios 100/0, 75/25, and 50/50 yielded the three molecular weight ranges 35 000, 40 000, and 190 000 listed in Table 1.) *N,N*-Dimethylacrylamide was dissolved in the desired solvent, and the solution was added to a predetermined quantity of *N*-(acryloxy)succinimide (see Table I) plus AIBN at 70 °C under nitrogen. The reaction mixture was stirred at 70 °C for 20 h. The polymer was precipitated by pouring the cooled solution into hexane.

1-(1-Pyrenyl)octadecane-Labeled Poly(*N,N*-dimethylacrylamide). The copolymer poly(*N,N*-dimethylacrylamide–*N*-(acryloxy)succinimide) was dissolved with the desired amount of 1-(1-pyrenyl)octadecylamine in tetrahydrofuran, a catalytic amount of triethylamine was added, the container was sealed, and the mixture was stirred overnight at room temperature. Subsequently, an excess of dimethylamine was added, the solution was stirred for an additional 3 h at room temperature, and the product was isolated by precipitation from hexane.

Polymer Hydrophobe Content. The final content of 1-(1-pyrenyl)octadecyl groups was determined using two independent techniques, UV spectroscopy and ^{1}H NMR spectroscopy. For UV measurements, a series of chloroform solutions of pyrene was used to obtain molecular extinction coefficients at the absorbance maxima occurring at 268, 278, 328, and 344 nm. The pyrene concentration of a solution containing a known amount of polymer dissolved in chloroform was then determined from its absorbance at those same wavelengths using the extinction coefficients of pyrene as a reference. For ^{1}H NMR spectra, the integrated intensity of the resonance lines assigned to the nine pyrenyl protons (7.95–8.50 ppm) was compared to that of the remaining resonances, for polymer dissolved in $CDCl_3$. This ratio remained constant provided a relaxation delay of at least 10 s was allowed.

Fluorescence Spectroscopy. Fluorescence spectra were recorded on a SLM 4800 spectrofluorometer (SLM Instruments, Inc.). Aqueous solutions (0.001–20 g/L) were prepared by allowing the polymer to dissolve in double-distilled water. Solutions were not degassed.[21] All measurements were carried out at 25 °C. Emission spectra were recorded with an excitation wavelength of 330 nm and slit widths of 8 nm (excitation) and 2 nm (emission). The excimer to monomer ratios were calculated by taking the ratio of the intensities at 450 nm to the intensities at 399 nm.

Pulsed-Gradient Spin-Echo NMR Spectroscopy. PGSE NMR measurements were performed using an MRI (magnetic resonance imaging) probe with actively shielded gradient coils (Doty Scientific, Columbia, SC) installed in a Chemagnetics CMX 300 NMR spectrometer operating at 300 MHz for protons. A standard Stejskal-Tanner PGSE sequence, $[(90°_x)$-τ-$(180°_y)$-$\tau]$ with gradient pulses during τ,[22] was employed. Particulars regarding the 90° pulse length (24 μs), interpulse delay (150 ms), recycle delay (4 s), spectral width (10 kHz), data size (8 K), line broadening (10 Hz), and number of acquisitions (8–2048 scans) are those noted in the parentheses unless stated otherwise. The PGSE experiments were performed at 23 °C, and the gradient pulse was applied to the z direction only. It was necessary to use several levels of gradient strength between circa 20 and 60 Gauss/cm, depending on the polymer concentration. The lower range of gradient strengths was calibrated by using the diffusion coefficient of 2 vol % H_2O in D_2O ($D = 1.9 \times 10^{-9}$ m^2/s)[23] (see eq 1 in the following section). In the case of higher gradients, a sample of 10 g/L poly(ethylene glycol) (PEG) in HDO, which could be measured with both low and high gradient strengths, was used as the calibration standard. The precision of the measured self-diffusion coefficients was good at low gradient strength; the error being estimated at less than 5%.

Viscosity Measurements. The viscosities of aqueous solutions of the various HM-PDMAM were measured using an Ostwald viscometer (0.3 mm diameter capillary, 2.0 mL capacity) immersed in a water bath maintained at 25 ± 0.2 °C. Flow-through times of HM-PDMAM solutions at various concentrations (1–20 g/L) were determined at least five times for each concentration. Specific viscosities ($\eta/\eta_0 - 1$) were determined by comparison with flow-through times of water ($\eta_0 = 0.89$ cP). The intrinsic viscosity $[\eta]$ was calculated from the intercept of a plot of $(\eta/\eta_0 - 1)/c$ versus concentration c.

Analytical Techniques. The molecular weights of the products of the polymerization reactions were determined using gel permeation chromatography (GPC) of the copolymer poly(*N,N*-dimethylacrylamide–*N*-(acryloxy)succinimide) which had been reacted with dimethylamine. The polymers were chromatographed in 0.1 M aqueous sodium nitrate on a system consisting of a Waters 590 HPLC pump connected to TSK gel

Table 1. Structural Features of Hydrophobically-Modified PDMAM Polymers

polymer designation	M_w[a]	M_w/M_n[a]	NMAM/NASI[b]	hydrophobes per chain[c]
HM-PDMAM/4.7	34 200	5.4	25/1	4.7
HM-PDMAM/2.3	33 800	5.4	50/1	2.3
HM-PDMAM/1.3	35 600	4.3	100/1	1.3
HM-PDMAM/0.7	37 700	5.0	150/1	0.72
HM-PDMAM/0.4	39 800	4.9	200/1	0.41
HM-PDMAM/4.8	48 400	6.7	25/1	4.8
HM-PDMAM/2.4	43 000	6.1	50/1	2.4
HM-PDMAM/1.6	44 800	6.6	100/1	1.6
HM-PDMAM/1.6	55 400	3.8	150/1	1.6
HM-PDMAM/1.2	60 000	5.1	200/1	1.2
HM-PDMAM/24	189 000	2.1	25/1	24
HM-PDMAM/13			50/1	13
HM-PDMAM/5.2			100/1	5.2
HM-PDMAM/3.3			150/1	3.3
HM-PDMAM/2.5			200/1	2.5

[a] Determined via GPC prior to hydrophobic modification. [b] *N,N*-Dimethylacrylamide/*N*-(acryloxy)succinimide in copolymerization vessel. [c] Determined via UV and ^{1}H NMR spectroscopy after hydrophobic modification.

G3000 PW and G5000 PW columns, with a Waters 486 UV monitor and a Waters R401 differential refractometer as detectors. Molecular weights were calculated by comparison to a polyacrylamide standard (80k) from Polysciences (Warrington, PA). Molecular weight polydispersity was calculated from the GPC trace. ^{1}H and ^{13}C NMR spectra were recorded on a Varian XL 400 NMR spectrometer operating at 400 and 100 MHz, respectively, in $CDCl_3$ solution containing tetramethylsilane as an internal chemical shift reference. Infrared spectra were recorded on a Nicolet 5-DXB FTIR with samples in the form of KBr disks. Ultraviolet spectra were recorded on a Hewlett Packard 8452A diode array spectrophotometer with samples dissolved in HPLC-grade chloroform.

Results

Polymer Characterization. The weight average molecular weights, molecular weight polydispersities, and the 1-(1-pyrenyl)octadecane content of the HM-PDMAM polymers synthesized for this study are listed in Table 1. Preliminary studies demonstrated that the molecular weight of the poly(*N,N*-dimethylacrylamide–*N*-(acryloxy)succinimide) copolymer could be varied by altering the ratio of *tert*-butyl alcohol/1-propanol used in the polymerization solvent. Three different molecular weight ranges were selected, and within each range a series of copolymers was synthesized in which the content of the *N*-(acryloxy)succinimide comonomer was progressively changed. Five ratios of NMAM/NASI, between 25/1 and 200/1, were selected from each molecular weight range.

Insolubility of the NASI comonomer in the polymerization solvent prevented attempts to achieve ratios higher than 25/1. GPC analysis showed that the differing amounts of NASI had some small effect on the molecular weight, with the general trend being for somewhat higher molecular weight at lower NASI contents. Solubility problems were encountered in most solvents, leading to the final choice of 0.1 M sodium nitrate for GPC analysis. Even so, with the highest molecular weight copolymers blocking of the GPC filters prevented our obtaining molecular weight data for all but one, as shown in Table 1. We feel, therefore, that the rather high polydispersities listed in Table 1 are more apparent than real and originate with this problem. We note that the GPC analysis was performed on the poly(NMAM–NASI) copolymer reacted with dimethylamine only and, therefore, containing no hydrophobic modifications.

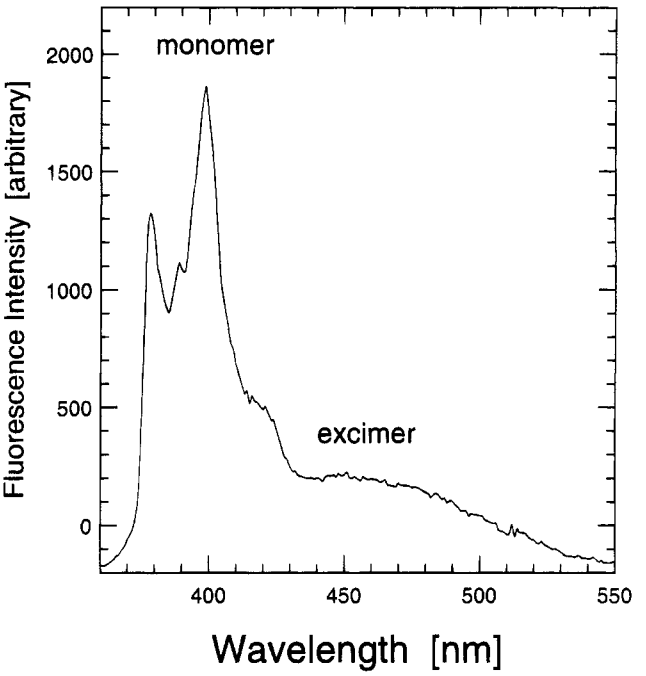

Figure 2. Typical fluorescence emission spectrum for a 20 g/L aqueous solution of the M_w 37 700 HM-PDMAM/0.7 polymer. The peaks at 378, 389, and 399 nm are assigned to pyrene monomer emission. The broad band centered at 450 nm is assigned to pyrene excimer emission.

The hydrophobe content of the various HM-PDMAM's was determined independently using UV spectroscopy and ^{1}H NMR spectroscopy, as described in the Experimental Section. The results listed in Table 1 are the average of the two independent values. In every case the hydrophobe contents determined by the two methods agreed quite closely with one another. It is evident that the hydrophobe content follows the trend expected from the ratio NMAM/NASI in the initial copolymerization.

The water solubility of the highest molecular weight HM-PDMAM polymers was so poor, regardless of the hydrophobe content, that no further characterization was attempted, and these polymers are omitted from Table 1. For the M_w 189 000 HM-PDMAM/24 and */13, their high hydrophobe content resulted in a limited water solubility which prevented further meaningful studies with these particular species. The designation "*/13" refers to the number of 1-(1-pyrenyl)octadecyl-containing segments per polymer chain.

Fluorescence Spectroscopy. Figure 2 shows a typical fluorescence spectrum for, in this instance, a 20 g/L aqueous solution of the M_w 37 700 HM-PDMAM/0.7 polymer. The fluorescence emission spectrum of excited pyrene in the absence of pyrene–pyrene interactions ("monomer" emission having intensity I_m) is characterized by a well-resolved spectrum consisting of major peaks at 378, 389, and 399 nm. Excimer formation occurs when an excited pyrene (Py*) and a pyrene in its ground state come into close proximity during the Py* lifetime. Pyrene excimer emission (intensity I_e) is characterized by a broad featureless spectral band centered at 450 nm. Hence, the ratio I_e/I_m has often been used as an indicator of the degree of interaction between fluorophores.[24] In this instance, the excimer/monomer ratio provides a measure of the degree of hydrophobic association between hydrophobically-modified sites on the polymer chain. Qualitatively, the fluorescence spectrum shown in Figure 2, where I_e/I_m

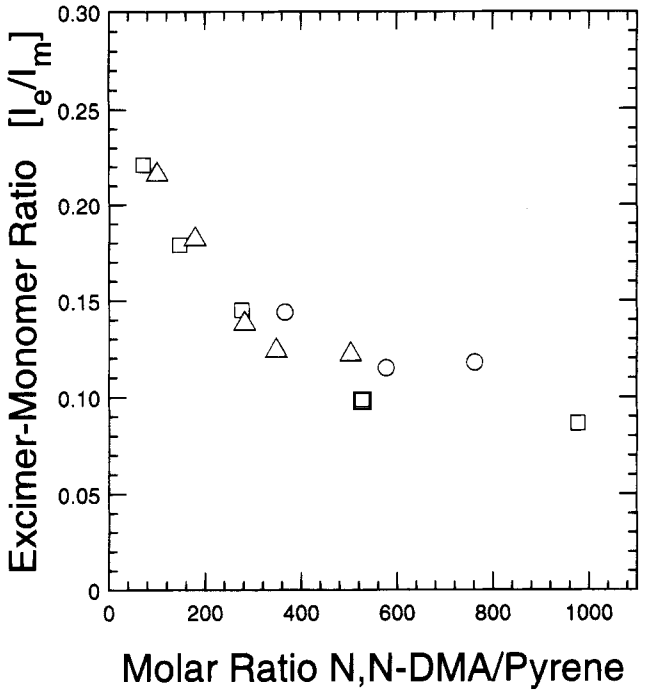

Figure 3. Excimer to monomer intensity ratio as a function of hydrophobe content for the three different molecular weight HM-PDMAM series at a constant concentration of 1.0 g/L: open boxes, M_w 35 000 series; open triangles, M_w 50 000 series; open circles, M_w 190 000 series.

equals 0.185, indicates that significant excimer formation occurs for this polymer at this concentration in aqueous solution. At higher pyrene concentrations various undesired side effects, such as self-quenching and reabsorption, may complicate the calculation of excimer to monomer ratios. In our spectra we observed that at the highest pyrene concentrations investigated (about 10^{-3} M) the intensity of the monomer peak at 378 nm diminishes noticeably relative to the intensity of the monomer peak at 399 nm; an effect attributable to reabsorption. In order to minimize any such effects we have chosen to calculate I_e/I_m as the ratio of peak intensities at 450 and 399 nm. Regarding the issue of "static" versus "dynamic" excimer formation, we have not performed fluorescence lifetime measurements and cannot resolve their relative contribution to the excimer intensity.

The first question we wished to address was whether the association phenomenon was most influenced by overall polymer molecular weight or by the hydrophobe content. Figure 3 shows a plot of I_e/I_m as a function of hydrophobe content for the three different molecular weight HM-PDMAM polymers at a constant concentration of 1.0 g/L. Excimer formation increases with increasing hydrophobe content in all cases. It is evident that the values of I_e/I_m for the different molecular weight HM-PDMAM's fall on a common curve. We conclude that for this particular hydrophobic moiety the association probability is largely independent of the polymer molecular weight and, instead, is determined mainly by the degree of hydrophobic modification of the polymer backbone.

On the basis of these findings regarding the molecular weight dependence of excimer formation, we chose to focus on one particular molecular weight and to investigate in detail that polymer's association properties as a function of hydrophobe content and concentration. Figure 4A illustrates the manner in which excimer

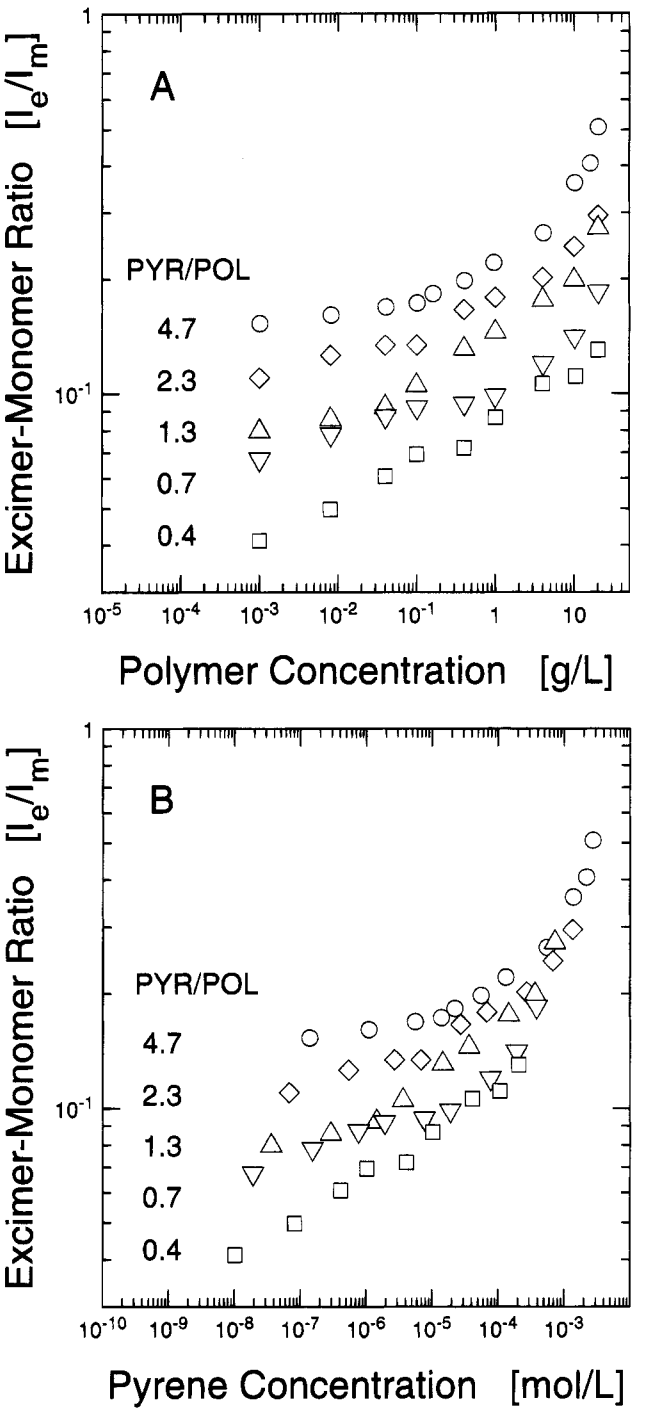

Figure 4. (A) Excimer to monomer intensity ratio as a function of polymer concentration for the five different hydrophobe content HM-PDMAM in the M_w 35 000 HM-PDMAM series: open boxes, 0.4 hydrophobe per chain; open reverse triangles, 0.7 hydrophobe per chain; open triangles, 1.3 hydrophobes per chain; open diamonds, 2.3 hydrophobes per chain; open circles, 4.7 hydrophobes per chain. (B) Excimer to monomer intensity ratio as a function of pyrene concentration for the five different hydrophobe content HM-PDMAM in the M_w 35 000 HM-PDMAM series. Symbol designations are identical to those in Figure 4A.

formation depends on polymer concentration for the five different hydrophobe contents of the M_w 35 000 HM-PDMAM series. At any given concentration the ratio I_e/I_m increases with increasing hydrophobe content, as noted in Figure 3. However, a comparison of the concentration dependence of excimer formation for the high versus low hydrophobe contents reveals two fundamentally different behaviors. For the case of the

lowest hydrophobe loading, in particular, excimer formation is insignificant at low concentrations and increases progressively with increasing concentration. For the case of the highest hydrophobe loading, in contrast, excimer formation occurs to a significant degree at low concentrations but remains almost independent of concentration until at the highest concentrations it begins to rise abruptly.

A more compelling demonstration of this difference in behavior for different hydrophobe loadings is obtained when one compares excimer formation on the basis of the absolute hydrophobe concentration, rather than absolute polymer concentration, as shown in Figure 4B. Here it becomes apparent that all polymers tend toward a common behavior at high hydrophobe concentrations but differ profoundly in their behavior at low hydrophobe concentrations. In particular, at low concentrations those polymers with low hydrophobe contents display a marked concentration dependence of excimer formation. In contrast, at similar low concentrations, for those polymers having a high hydrophobe content, excimer formation is virtually independent of concentration. We interpret this difference as indicating that high hydrophobe content polymers prefer intramolecular over intermolecular associations at low concentrations.

Pulsed-Gradient Spin-Echo NMR. The PGSE NMR pulse sequence consists of a pair of magnetic field gradient pulses (duration δ and amplitude G), the first being applied between the two radio-frequency (rf) pulses of the usual spin-echo NMR sequence and the second between the last rf pulse and the appearance of the spin-echo signal. For isotropic diffusion characterized by a single diffusion coefficient, in a homogeneous magnetic field where the residual gradient G_0 is negligible, the intensity, $I_{2\tau}$, of the NMR signal at time 2τ following the start of the PGSE pulse sequence is related to the diffusion coefficient D_0 as per eq 1, where G is

$$I_{2\tau} = I_0 \exp[-(\gamma G\delta)^2(\Delta - \delta/3)D_0] \qquad (1)$$

the pulsed-gradient strength, δ is the duration of the gradient, Δ is the interval between the gradients, τ is the rf pulse interval, and γ is the magnetogyric ratio.[22] The effect of T_2 (spin−spin relaxation time) is constant when τ is kept constant and is contained within the term I_0. The diffusion coefficient can be derived from the slope of a plot of the logarithm of the signal intensity as a function of $\delta^2(\Delta - \delta/3)$ once the gradient strength G is known. The latter is obtained by calibration with a sample of known diffusion coefficient, as described previously.

Figure 5 shows a series of ^{1}H NMR spectra of the M_w 34 200 HM-PDMAM/4.7 polymer at 10.0 g/L in D_2O, for various durations of the field gradient pulse. The leftmost spectrum was obtained with a very short gradient pulse and shows two resonances, one arising from the residual protons in heavy water and the other from the methyl protons of the *N,N*-dimethyl group. Other expected resonances, such as those of the dimethylacrylamide backbone or the methylenes of the octadecyl moiety or the aromatic protons of the pyrenyl group, do not appear, either because of their small numbers relative to the methyl protons or because of their shorter spin−spin (T_2) relaxation times relative to the methyl protons. Note that all the expected resonances are readily apparent in the ^{1}H NMR spectra of the HM-PDMAM's in chloroform. If the associated state which

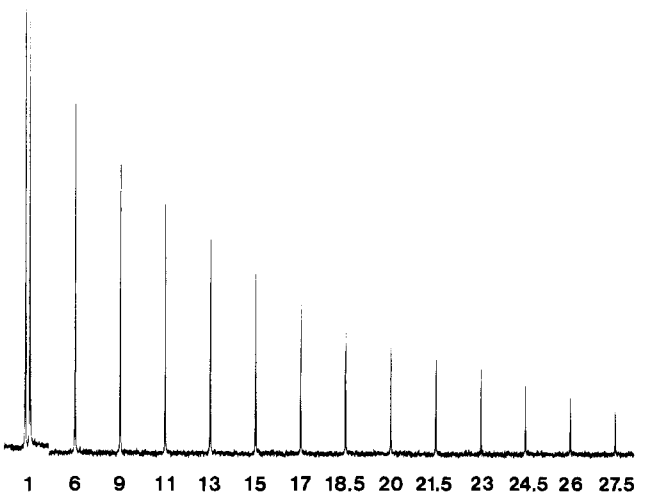

Figure 5. Series of proton PGSE NMR spectra of M_w 34 200 HM-PDMAM/4.7 at 10 g/L in deuterium oxide at room temperature, showing the attentuation of the proton signals with increasing duration of the gradient pulse δ, indicated in milliseconds. In this instance the gradient pulse amplitude (G) was 58 Gauss/cm while the gradient interpulse duration (Δ) was 150 ms.

forms in aqueous solution involves hindered molecular motion, such as would be expected within a micellar cluster, then T_2 shortens and the NMR line width increases. Thus, for the τ value used in these measurements (150 ms), the resonance signals of the 1-(1-pyrenyl)octadecyl hydrophobic modifiers may well be largely suppressed. The methylene and methyne protons of the dimethylacrylamide backbone are not observed in the PGSE NMR experiment, even for PDMAM control polymers lacking any hydrophobic modifications whatsoever (data not shown). Their absence from the spectrum is likely due, therefore, to motional effects on T_2 arising from stiffness of the backbone rather than any specific effect of hydrophobic modification. With increasing gradient pulse duration, the HDO resonance intensity quickly decreases to zero, which is anticipated given the rapid diffusion of water and the rather high gradient strengths used in this particular experiment. For longer gradient pulse durations, only the *N*-methyl resonance signal remains and its intensity decays exponentially with increasing duration of the gradient pulse.

Figure 6A shows a typical plot of the logarithm of the signal intensity of the acrylamide methyl protons as a function of the gradient pulse duration, in this instance for the M_W 34 200 HM-PDMAM/4.7 polymer at 10.0 g/L. The intensity decay shown in Figure 6A is quite evidently multi-exponential, implying a dispersion of effective diffusion coefficients. The possible origins of such a distribution of diffusion coefficients include restricted diffusion and polydispersity of size.[17,25] One method for analyzing such a multi-exponential decay is to use a "stretched exponential" of the form shown in eq 2.[9] The parameter β is a measure of the width of

$$I_{2\tau} = I_0 \exp -\{[(\gamma G\delta)^2(\Delta - \delta/3)D_e]^\beta\} \qquad (2)$$

the distribution of diffusion coefficients, and $0 \le \beta \le 1$, so that for a monodisperse diffusion coefficient $\beta = 1$ and eq 2 reverts to eq 1. The parameter D_e is an effective self-diffusion coefficient, which is related to the mean diffusion coefficient, D_m, via the gamma function, Γ, according to eq 3, where $X = (\gamma G\delta)^2(\Delta - \delta/3)$. Ideally,

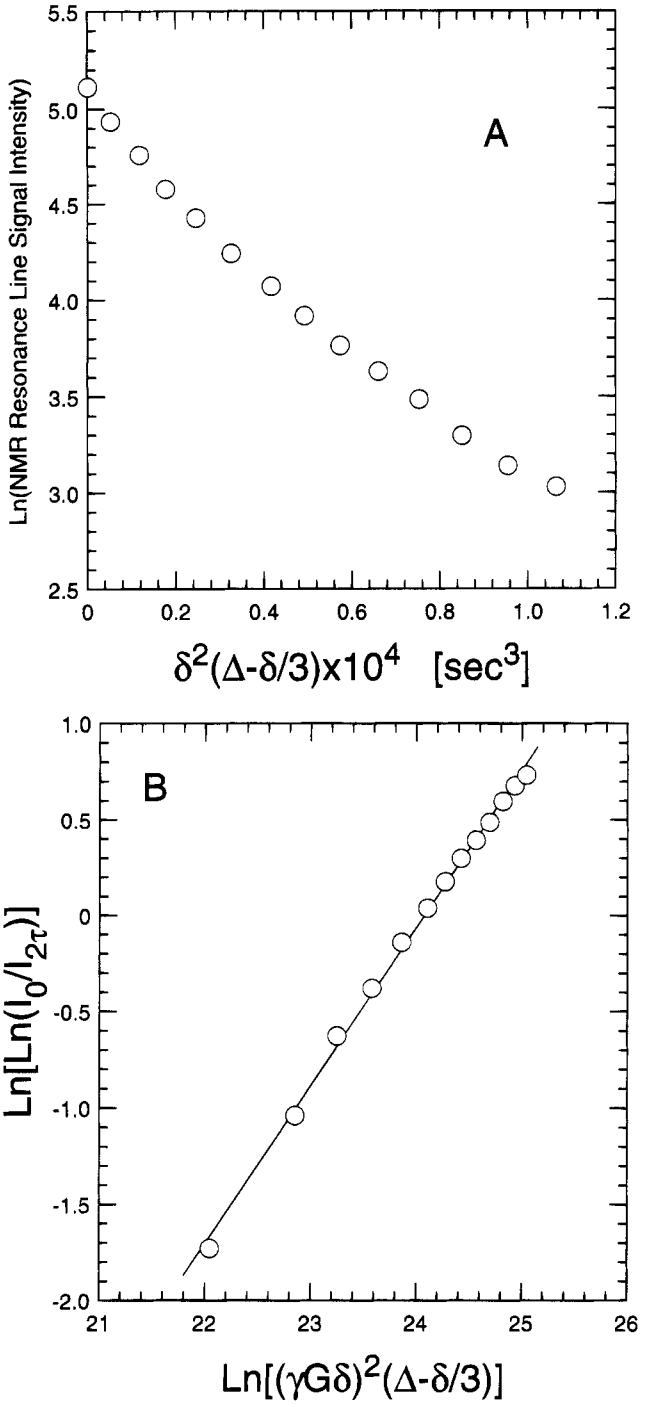

Figure 6. (A) Typical plot of the logarithm of the signal intensity of the acrylamide methyl protons as a function of $\delta^2(\Delta - \delta/3)$ for M_w 34 200 HM-PDMAM/4.7 at 10 g/L in deuterium oxide. (B) Determination of the width of the distribution of diffusion coefficients (β) and the effective diffusion coefficients (D_e) using a linearized version of eq 2. β corresponds to the slope while the intercept corresponds to β ln D_e. The data points are those in Figure 6A, while the solid line is fit using eq 2 with the slope and intercept noted in the text.

$$\frac{1}{D_m} = \int_0^\infty \exp\{-(XD_e)^\beta\}\, dX = (1/\beta)(1/D_e)\Gamma(1/\beta) \quad (3)$$

β and D_e are obtained from a two-parameter nonlinear least squares fit of eq 2 to the diffusion data. However, values for β and D_e can also be estimated by plotting ln[ln($I_0/I_{2\tau}$)] versus ln(X), which should be linear with slope equal to β and intercept equal to β ln(D_e). Figure 6B shows the results of such an analysis of the data shown in Figure 6A. In this case values of β and D_m equal 0.821 and 3.13×10^{-11} m^2 s^{-1}.

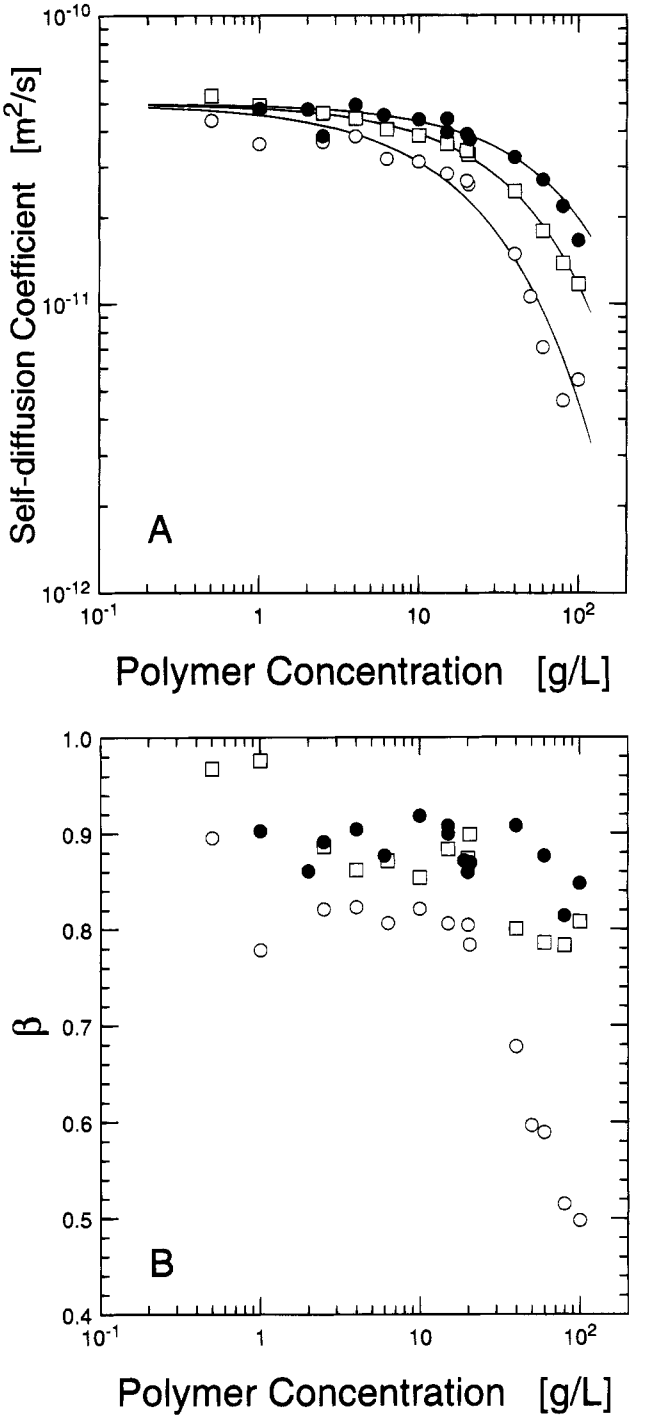

Figure 7. (A) Mean self-diffusion coefficient as a function of concentration for two HM-PDMAM polymers and the control PDMAM polymer: open circles, M_w 34 200 HM-PDMAM/4.7 (high degree of hydrophobic modification); open boxes, M_w 39 800 HM-PDMAM/0.4 (low degree of hydrophobic modification); closed circles, M_w 35 000 PDMAM (no hydrophobic modifications). (B) Distribution of diffusion coefficients about mean values as a function of concentration for the same three polymers in Figure 7A. Symbol designations are identical to those in Figure 7A.

Figure 7A compares the concentration dependence of the mean self-diffusion coefficients of three polymers: one having a high degree of hydrophobic modification (M_w 34 200 HM-PDMAM/4.7), one having a low degree

of hydrophobic modification (M_w 39 800 HM-PDMAM/0.4), and one lacking hydrophobic modifications altogether (M_w 35 000 PDMAM). The diffusion coefficients of the control polymers lacking hydrophobic modifiers are remarkably similar to those of poly(ethylene oxide) of similar molecular weight and manifest the same relatively weak dependence on polymer concentration.[10] A pronounced effect of even low levels of hydrophobic modification is to decrease the diffusion coefficient relative to the control polymer, and this effect becomes even more pronounced with increasing polymer concentration. For the polymer having a high degree of hydrophobic modification, even at low concentrations the diffusion coefficients are substantially reduced relative to the controls, while the concentration dependence itself is even more exaggerated.

The parameter β is a measure of the width of the distribution about the mean self-diffusion coefficient. One must recognize that using a stretched exponential to describe the magnitude of the dispersion of diffusion coefficients may actually obscure details regarding the nature of the dispersion. Indeed, it is possible to obtain identical values of β for particular continuous and biphasic dispersions. Provided these limitations are kept in mind when employing such an approach, its application can prove useful. For instance, at low polymer concentrations values of β approach unity for all cases, as shown in Figure 7B, indicating a rather narrow distribution of self-diffusion coefficients. Deviations from unity on this order may be accounted for largely in terms of the polydispersity of polymer size.[25] For the control polymer, β remains constant with increasing concentration, within the error of the determination. The low hydrophobe-containing polymer behaves in a similar fashion. But with the high hydrophobe-containing polymer, β is clearly smaller at all concentrations relative the other polymers and decreases progressively at the highest concentrations investigated.

The PGSE NMR diffusion coefficient measurements indicate that increasing hydrophobe content and polymer concentration causes polymer diffusion to decrease and the dispersion of diffusion coefficients about the mean value to increase. Undoubtedly, these effects are a manifestation of the same hydrophobic associations evident from the fluorescence measurements of excimer/monomer ratios. One would like to extract from the diffusion measurements an estimate of the average size of any associated cluster and the number of polymers of which it is composed. However, the diffusion coefficient is a function of both the size of the diffusing unit and the solution viscosity. Therefore, before interpreting the diffusion data further, one must perform corresponding viscosity measurements.

Viscosity Measurements. The relative viscosities for solutions of the same three polymers investigated via PGSE NMR are shown in Figure 8, where in the usual fashion one plots $(\eta/\eta_0 - 1)/c$ versus c. At any given concentration the specific viscosity $(\eta/\eta_0 - 1)$ of the low-hydrophobe-content polymer solutions was higher than that of the control polymer. Conversely, the high-hydrophobe-content polymer always yielded specific viscosities lower than those of the control polymer. Over the concentration range investigated no transition to a different dependence of viscosity on concentration was observed for any of the three polymers. The intrinsic viscosity $[\eta]$, listed in Table 2, is obtained from the intercept at zero concentration and, given the linearity

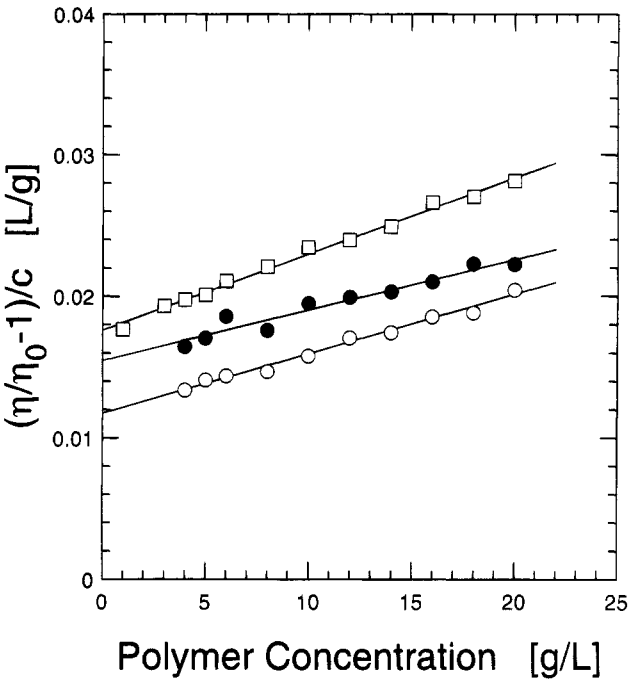

Figure 8. Determination of the intrinsic viscosity from $(\eta/\eta_0 - 1)/c$ as a function of concentration for two HM-PDMAM polymers and the control PDMAM polymer: open circles, M_w 34 200 HM-PDMAM/4.7 (high degree of hydrophobic modification); open boxes, M_w 39 800 HM-PDMAM/0.4 (low degree of hydrophobic modification); closed circles, M_w 35 000 PDMAM (no hydrophobic modifications).

Table 2. Physical Properties of Hydrophobically-Modified PDMAM Polymers

	polymer designation		
property	PDMAM M_w 35 000	HM-PDMAM/0.4 M_w 39 800	HM-PDMAM/4.7 M_w 34 200
D_0 (10^{-11} m^2 s^{-1})	4.88	5.25	3.98
R_h (nm)	5.03	4.67	6.17
$[\eta]$ (L g^{-1})	0.0155	0.0176	0.0118
n	1.4	0.9	3.7
α (wt %)	0.154	0.264	0.505
γ	0.812	0.775	0.705
c^*_{diff} (g L^{-1})	70	34	34
c^*_{geo} (g L^{-1})	59	81	121

of these plots, the values have good precision. Again, the intrinsic viscosity of the low-hydrophobe-content polymer was larger than that of the control polymer, while the high-hydrophobe-content polymer was lower.

The intrinsic viscosity may be used to estimate a cluster size number for the associated state according to eq 4, where n is the number of polymer molecules

$$[\eta](nM) = (10\pi/3)N_A R_h^3 \quad (4)$$

constituting an associated cluster, M is the polymer molecular weight, N_A is Avogadro's number, and R_h is the hydrodynamic radius determined from diffusion measurements. The latter value is obtained using the Stokes–Einstein relationship as shown in eq 5, where

$$R_h = kT/6\pi\eta D_0 \quad (5)$$

η is the solution viscosity and kT is the Boltzmann temperature. If one extrapolates the concentration dependence of the diffusion coefficients back to infinite dilution to obtain D_0 (listed in Table 2) and assumes that the viscosity equals that of pure water, then applying eq 5 one finds hydrodynamic radii equal to 6.2,

4.7, and 5.0 nm for the high-hydrophobe-content, low-hydrophobe-content, and control polymers, respectively. Employing eq 4 then yields cluster size numbers of approximately 4, 1, and 1, for the high-hydrophobe-content, low-hydrophobe-content, and control polymers, respectively. With increasing concentration the cluster size numbers remain constant for the two different HM-PDMAM's and for the control PDMAM.

It is important to emphasize that the lowest concentration accessible with PGSE NMR or viscosity measurements is still far greater than that accessible with fluorescence measurements. Consequently, extrapolating PGSE NMR data to infinite dilution takes no account of possible transformation occurring at lower concentrations.

Discussion

The combined fluorescence–PGSE NMR–viscosity results may be summarized as follows. In general, higher degrees of hydrophobic modification cause higher polymer association probabilities. More specifically, at low degrees of hydrophobic modification the degree of association is highly concentration dependent at all concentrations, while at high degrees of hydrophobic modification there is a crossover with increasing polymer concentration from a concentration-independent to a concentration-dependent behavior. Network formation does not occur within the range of concentrations investigated. In the concentration range accessible to PGSE NMR, the most hydrophobically-modified polymers form clusters consisting of four macromolecules on average.

HM-PDMAM Fluorescence. Previous fluorescence studies of both randomly-hydrophobically-modified[16] and end-cap hydrophobically-modified polymers[26,27] have been interpreted as indicating a crossover from intramolecular to intermolecular associations with increasing polymer concentration. The fluorescence behavior shown in Figure 4A suggests that a similar interpretation is warranted in the case of the HM-PDMAM studied here. Associations are driven energetically by favorable hydrophobic attractions, which outweigh unfavorable chain configurational restrictions. Thus, excimer/monomer ratios in the fluorescence spectrum are an indicator of the degree of hydrophobic association. At high polymer concentrations, intermolecular associations will be favored statistically regardless of the degree of hydrophobic modification, so that excimer formation, and excimer/monomer ratios, will increase with increasing concentration. At low polymer concentrations, polymers having a high degree of hydrophobic modification will still have the opportunity to undergo intramolecular excimer formation, but excimer/monomer ratios will become almost concentration independent. For polymers having a low degree of hydrophobic modification, the opportunity to undergo intramolecular excimer formation is precluded, and excimer/monomer ratios will continue to decrease with decreasing concentration.

It is possible to construct and parameterize a simple intramolecular versus intermolecular equilibrium association model for polymers having defined degrees of hydrophobic modification yielding excimer/monomer ratios as a function of polymer concentration which emulate the behavior shown in Figure 4 (Uemura, McNulty, and Macdonald, unpublished results). However, any such model provides at best a qualitative guide to the association events underlying the observed dependence of excimer formation on polymer concentration and hydrophobe content. Quantitative comparisons are unwarranted. In particular, the proportionality constants relating the observed fluorescence to amounts of monomer versus excimer are unknown. Likewise, the relative contributions of "static" versus "dynamic" excimer formation are unknown. We consider it most likely that we are observing "static" excimer formation. However, only further measurements, either time-resolved fluorescence or excitation spectra for the monomer versus excimer fluorescence, could resolve the question definitively. Furthermore, the hydrophobe content of the various HM-PDMAM polymers is only known on average. Thus, the M_w 39 800 HM-PDMAM/0.4 polymer, for example, assuming a Poisson distribution, consists of 66% unmodified, 27% singly-modified, and 6% doubly-modified fractions. Moreover, one would need to account for the possible influence of the random distribution of hydrophobes along the polymer chain, and the polydispersity of polymer size. Finally, one should give consideration to association sites consisting of multiple hydrophobes, or aggregates of multiple polymer chains. Under experimental circumstances in which uncertainties regarding the number of hydrophobes per polymer chain and their location were minimized, it should be possible to extract from fluorescence data information regarding hydrophobe aggregation numbers and polymer cluster sizes for such hydrophobically-modified polymers. An example of such a simplified topology of hydrophobic modifications are the telechelic HEUR thickeners.

HM-PDMAM Self-Diffusion. An overview of the PGSE polymer self-diffusion results can be obtained using a recently developed hydrodynamic scaling model for polymer self-diffusion.[28] According to this model, the self-diffusion coefficient at any particular concentration, D_c, is related to the self-diffusion coefficient at infinite dilution, D_0, as per eq 6, where α and γ are the corresponding scaling parameters. The best-fit values of these scaling parameters for the two HM-PDMAM and the control PDMAM polymers are listed in Table 2, for the case in which it is assumed that the self-diffusion coefficients at infinite dilution are identical for all three polymers. The solid lines in Figure 7A were calculated using eq 6, and the parameters are listed in Table 2. The relative tendency to associate is manifest in the values of both α and γ which tend to increase and decrease, respectively, with increasing hydrophobe content.

$$D_C = D_0 \exp(-\alpha c^{\gamma}) \tag{6}$$

Another measure of these polymers' association tendency which may be obtained from PGSE NMR self-diffusion data involves comparing the calculated geometrical overlap concentration, c^*_{geo}, with that observed from diffusion measurements, c^*_{diff}, as determined from the inflection point in a plot of $1/D$ versus concentration. From the values of these quantities listed in Table 2 it is evident that for the control PDMAM polymer c^*_{diff} and c^*_{geo} are approximately equal, while for the two HM-PDMAM polymers the ratio c^*_{diff}/c^*_{geo} is less than unity, the effect being greater with higher hydrophobe content. Effectively, the hydrophobes lower the apparent overlap concentration relative to that predicted from classical hydrodynamic theory; an effect attributable to associations induced by their presence.

The PGSE NMR plus viscosity data indicate the associated states induced by the random octadecylpyre-

nyl hydrophobic modifiers consist of small clusters and that gelation is not observed. This behavior is distinctly different from that observed with telechelic hydrophobically-modified polymers, such as the HEUR thickeners. When the hydrophobic modifications are located strictly at each end of the polymer chain, increasing the polymer concentration causes micellization and eventually cross-linking of micelles to form a gel which spans the entire solution. The apparent overlap concentration c^*_{diff} for the HEUR thickeners is about 1 order of magnitude lower than that of the HM-PDMAM's.[8-10] Likewise, the hydrodynamic scaling parameter α is consistently lower for the HM-PDMAM relative to the HEUR thickeners.[8-10] Both these measures of the tendency to associate indicate, therefore, that telechelic hydrophobic modifications are superior to random hydrophobic modifications in producing gelation.

Theory suggests, however, that randomly-hydrophobically-modified, or "comblike", associating polymers may show a variety of association behaviors, characterized by phenomena such as gelation, strong shear-thinning, or shear-induced gelation.[11,29] Indeed, McCormick *et al.*[30] showed that clear gelation occurs in aqueous solutions of acrylamide/*N*-alkylacrylamide copolymers, which have a comblike hydrophobe distribution. These particular acrylamide/*N*-alkylacrylamide copolymers were prepared by micelle polymerization, which produces a blocky distribution of hydrophobes. The corresponding copolymers prepared by homogeneous polymerization, which produces a more random distribution of hydrophobes, did not show any gelation in water. Another independent report[31] confirmed that acrylamide/*N*-alkylacrylamide copolymer prepared by homogeneous polymerization showed no gelation under almost the same conditions as McCormick's. Thus we conclude that a random distribution of hydrophobic modifications is unfavorable for network formation and gelation. Nevertheless, such polymers interact strongly with surfactants,[30-32] latex particles,[33] and lipid vesicles,[34] and it will be of interest to characterize these interactions via PGSE NMR self-diffusion measurements.

References and Notes

(1) *Water Soluble Polymers*; Glass, J. E., Ed.; Advances in Chemistry Series No. 213; American Chemical Society: Washington, DC, 1986.
(2) *Polymers in Aqueous Media*; Glass, J. E., Ed.; Advances in Chemistry Series No. 223; American Chemical Society: Washington, DC, 1989.
(3) *Polymers as Rheology Modifiers*; Schulz, D. N., Glass, J. E., Eds.; ACS Symposium Series 462; American Chemical Society: Washington, DC, 1991.
(4) Yekta, A.; Duhamel, J.; Adiwidjaja, H.; Brochard, P.; Winnik, M. A. *Langmuir* **1993**, *9*, 881.
(5) Nyström, B.; Walderhaug, H.; Hansen, F. K. *J. Phys. Chem.* **1993**, *97*, 7743.
(6) Winnik, F. M.; Ringsdorf, H.; Venzmer, J. *Langmuir* **1991**, *7*, 905.
(7) Winnik, F. M.; Ringsdorf, H.; Venzmer, J. *Langmuir* **1991**, *7*, 912.
(8) Persson, K.; Abramsen, S.; Stilbs, P.; Hansen, F. K.; Walderhaug, H. *Colloid Polym. Sci.* **1992**, *270*, 465.
(9) Walderhaug, H.; Hansen, F.; Abramsen, S.; Persson, K.; Stilbs, P. *J. Phys. Chem.* **1993**, *97*, 8336.
(10) Rao, B.; Uemura, Y.; Dyke, L.; Macdonald, P. M. *Macromolecules* **1995**, *28*, 531.
(11) Annable, T.; Buscall, R.; Ettelaie, R.; Whittlestone, D. *J. Rheol.* **1993**, *37*, 695.
(12) Maechling-Strasser, C.; Clouet, F.; Francois, J. *Polymer* **1992**, *33*, 1021.
(13) Groot, R. D.; Agterof, W. G. M. *J. Chem. Phys.* **1994**, *100*, 1649.
(14) Groot, R. D.; Agterof, W. G. M. *J. Chem. Phys.* **1994**, *100*, 1657.
(15) Jenkins, R. D. Ph.D. Thesis, Lehigh University, Bethlehem, PA, 1990.
(16) *Water Soluble Polymers*; Shalaby, S. W., McCormick, C. L., Butler, G. B., Eds.; ACS Symposium Series 467; American Chemical Society: Washington DC, 1991.
(17) Stilbs, P. *Prog. Nucl. Magn. Reson. Spectrosc.* **1987**, *19*, 1.
(18) Winnik, F. M. *Polymer* **1990**, *31*, 2125.
(19) Hutchins, R. O.; Hutchins, M. K. In *Comprehensive Organic Synthesis*; Trost, B. M., Fleming, I., Eds.; Pergamon Press: Oxford, U.K., 1991; Vol. 8, p 25.
(20) *Friedel-Crafts and Related Reactions*; Olah, G., Ed.; Wiley Interscience: New York, 1963; Vol. 3, p 78.
(21) Parker, C. A.; Hatchard, C. G. *Trans. Faraday Soc.* **1963**, *59*, 284.
(22) Stejskal, E. O.; Tanner, J. E. *J. Chem. Phys.* **1965**, *42*, 288.
(23) Mills, R. *J. Phys. Chem.* **1973**, *77*, 685.
(24) Winnik, F. M. *Chem. Rev.* **1993**, *93*, 587.
(25) Von Meerwall, E. D. *Adv. Polym. Sci.* **1983**, *54*, 1.
(26) Char, K.; Frank, C. W.; Gast, A. P.; Tang, W. T. *Macromolecules* **1987**, *20*, 1833.
(27) Richey, B.; Kirk, A. B.; Eisenhart, E. K.; Fitzwater, S.; Hook, J. *J. Coat. Technol.* **1991**, *63*, 31.
(28) Phillies, G. D. J. *J. Phys. Chem.* **1989**, *93*, 5029.
(29) Ballard, M. J.; Buscall, R.; Waite, F. A. *Polymer* **1988**, *29*, 1287.
(30) McCormick, C. L.; Nonaka, T.; Johnson, C. B. *Polymer* **1988**, *29*, 731.
(31) Effing, J. J.; McLennan, I. J.; Kwak, J. C. T. *J. Phys. Chem.* **1994**, *98*, 2499.
(32) di Meglio, J.-M.; Baglioni, P. J. *Phys. Chem.* **1994**, *98*, 5478.
(33) Jenkins, R. D.; Durali, M.; Silebi, C. A.; El-Aasser, M. S. *J. Colloid Interface Sci.* **1992**, *154*, 502.
(34) Ringsdorf, H.; Venzmer, J.; Winnik, F. M. *Angew. Chem.* **1991**, *30*, 315.

MA946187U